

# Synthesis of poly(HEMA-co-AAm) hydrogels by visible-light photopolymerization of aqueous solutions containing aspirin or ibuprofen: analysis of the initiation mechanism and the drug release

María Lorena Gómez<sup>a\*</sup>, Antonela Gallastegui<sup>a</sup>, Mariana B. Spesia<sup>a</sup>, Hernán A. Montejano<sup>a</sup>, Roberto J. Williams<sup>b</sup> and Carlos M. Previtali<sup>a</sup>

Recently, we reported the synthesis of hydrogels by visible-light photopolymerization of 2-hydroxyethylmethacrylate and acrylamide, employing safranin O as sensitizer, and a functionalized silsesquioxane (SFMA) as co-initiator/crosslinker. The influence of the ionic character of a drug on its release rate from the hydrogels was also reported. In the present study, we analyzed the photoinitiation mechanism, the synthesis of hydrogels in the presence of aspirin (ASA) or ibuprofen (Ibu), and their release from hydrogels synthesized with variable SFMA concentrations. Concerning the photoinitiation mechanism, we found that the main contribution was the electron transfer reaction between the excited triplet state of safranin and SFMA, followed by a fast proton transfer reaction from secondary amine groups. The generated nitrogen radicals initiated the copolymerization reaction. The photo-reaction quantum yield was 0.031. Concerning the drug-release study, we found that the release rate of both drugs increased by increasing pH from 7 to 10. This was ascribed to the increase in the partial ionization of the carboxylic acid groups, a fact that reduced the interactions with the secondary amine groups present in SFMA and increased the release rate. The effect was larger for ASA than for Ibu. Increasing the amount of SFMA increased both the crosslink density and the fraction of H-bonds formed with the drugs. At pH 10, the increment in the crosslink density was dominant for the release of Ibu while the increase in fraction of H-bonds determined the release rate of ASA. Cytotoxicity studies showed that these materials did not exhibit significant hemolytic activity. Copyright © 2016 John Wiley & Sons, Ltd.

**Keywords:** hydrogels; silsesquioxane; photopolymerization; aspirin; ibuprofen

## INTRODUCTION

Analgesics and nonsteroidal anti-inflammatory drugs (NSAIDs) are among the most commonly used therapeutic groups worldwide.<sup>[1]</sup> Among their adverse effects, the most common are the propensity to induce gastric or intestinal ulcers, sometimes accompanied by anemia.<sup>[2,3]</sup> These adverse effects may occasionally be inseparable from desired effects. Side effects are often dose-dependent and time-treatment dependent.<sup>[4]</sup> One way to avoid these drawbacks is through the employment of controlled drug release systems. These facilitate the delivery of drugs in moderate doses under controlled conditions.

Important efforts have been directed toward the development of diverse systems for a better encapsulation and release of drugs.<sup>[5–8]</sup> A broad variety of materials, such as micelles, liposomes, hydrogels (HGs), polymeric nanoparticles, molecular imprinted polymers, etc., has been used to this end. Among these, HGs are particularly suitable for a wide variety of applications in the medical and pharmaceutical industry due to their excellent biocompatibility and stability.<sup>[9]</sup> HGs are a particular class of crosslinked polymers that, due to their hydrophilic nature, can absorb large quantities of water without dissolving. These materials possess mechanical, physical, and chemical stability in their

swollen state, properties that have made them useful in various biomedical applications.<sup>[10,11]</sup> Smart HGs that respond to various stimuli such as pH, temperature, salinity, electric field, etc., have been reported.<sup>[12,13]</sup>

\* Correspondence to: María Lorena Gómez, Departamento de Química, Universidad Nacional de Río Cuarto y CONICET, Campus Universitario, 5800 Río Cuarto, Argentina.  
E-mail: mlgomez@exa.unrc.edu.ar

a M. L. Gómez, A. Gallastegui, M. B. Spesia, H. A. Montejano, C. M. Previtali  
Departamento de Química, Universidad Nacional de Río Cuarto y CONICET, Campus Universitario, 5800, Río Cuarto, Argentina

b R. J. Williams  
Instituto de Investigaciones en Ciencia y Tecnología de Materiales (INTEMA), Universidad Nacional de Mar del Plata, CONICET, J. B. Justo 4302, 7600, Mar del Plata, Argentina

**Abbreviations used:** AAm, acrylamide; ASA, aspirin; CFR, cumulative fractional release; HEMA, 2-hydroxyethylmethacrylate; HG, hydrogel; HRB, human red blood; Ibu, ibuprofen; NSAID, nonsteroidal anti-inflammatory drug; Saf, safranin O; SFMA, silsesquioxane functionalized with methacrylate and amine groups; Sw, swelling.



of Saf/SFMA in similar proportions as in our previous study.<sup>[20]</sup> Typically, 3 mL of a deoxygenated aqueous solution (50% by volume) of this formulation was irradiated for 3 hr at 20°C in a homemade merry-go-round photochemical reactor supplied with 12 green light-emitting diodes (LEDs) (73 mW,  $\lambda_{\max}$  530 nm). ASA or Ibu was incorporated to the initial solution before irradiation. A concentration of 0.01 g/mL was employed for both drugs. Irradiation was carried out until complete conversion was reached. After stopping the irradiation, tubes were kept for 48 hr in the dark. Then, the HGs were extracted by breaking the tubes. Samples cut as uniform disks of 10.5 mm diameter and 2.5 mm thickness (~0.1 g) were dried in an oven at 40°C for 48 hr.

### Swelling

Dried disks were weighed and immersed in commercial buffer solutions in an oven at 25 and 40°C ± 2°C. At specified times, the samples were removed from the solutions, blotted with filter paper to eliminate excess of solution, and weighed ( $W_t$ ). Then, they were immersed again in the buffer solution and returned to the oven. Three samples were used per point of the swelling curve. The degree of swelling ( $S_w$ ) was calculated as:

$$S_w = \frac{(W_t - W_0)}{W_0} = k_p t^{n_p} \quad (1)$$

where  $W_0$  represents the weight of the dried HGs (before swelling) and  $k_p$  and  $n_p$  are the kinetic constant of water diffusion into the network and the swelling exponent (which depends on the diffusion mechanism), respectively.

### Loading and release of drugs

Release experiments were carried out by transferring the dried drug-loaded disks into 10 mL buffer solutions of different pHs at 25°C. At specified time intervals, 3 mL aliquots were removed from every solution (three aliquots of different solutions for any single point of the release curve) and their absorbance was determined by UV-Vis spectroscopy (HP 8452 A, Hewlett-Packard) at the maximum absorption wavelength of each drug (296 nm for ASA and 273 nm for Ibu). After measuring the absorbance, aliquots were returned to the original solutions to keep volume constant. Calibration curves were used to transform absorbance determinations into concentrations. The samples were placed in a 1 × 1 × 3 cm quartz cell and spectra recorded at 25°C.

The experimental results were adjusted by an empiric equation developed by Ritger and Peppas<sup>[21]</sup>:

$$CFR = \frac{M_t}{M_\infty} = kt^n \quad (2)$$

where  $CFR$  represents controlled fractional released,  $M_\infty$  represents the amount of drug that was loaded to the HG (in mass per unit mass of polymer), and  $M_t$  corresponds to the amount of drug released at time  $t$ .  $k$  is a constant, and  $n$  is the diffusional exponent characteristic of the release mechanism.

### Photochemical and characterization techniques

Absorption spectra were obtained by using a Hewlett-Packard 8453 diode array UV-Vis spectrophotometer. Steady state photolysis was carried with the same illuminating system employed for the synthesis of HGs at  $\lambda_{\max}$  = 530 nm. Experiments were

performed at 25 ± 0.5°C. Aberchrome 540 from Aberchromics LTD in toluene was used as actinometer. The fluorescence spectra were determined with a Spex Fluoromax spectrofluorometer. Fluorescence lifetimes were determined by time-correlated single photon counting by using an OB 900 Edinburgh Instruments spectrofluorometer. Triplet-triplet absorption spectra and triplet lifetimes were determined by using the experimental setup described in previous papers.<sup>[22]</sup> Excitation of the dye was carried out at 532 nm by using the second harmonic of an Nd-YAG laser. A flow cell was used in order to avoid photodecomposition of Saf in the presence of SFMA.

To visualize the pore structure of the HG in the swollen state, a JEOL JSM-6460 LV scanning electron microscope (SEM)—from Jeol Technics Ltd., Tokyo, Japan—was employed. The samples were swollen to equilibrium, maintaining them 24 hr in buffer solutions, blotted with filter paper, frozen at -18°C, and freeze-dried for 24 hr in a Virtis Benchtop SLC, SP Industries, New York, USA. Freeze-dried samples were loaded on the surface of an aluminum SEM specimen holder and sputter coated with Au-Pd for 35 sec before observation. A working distance about 20–25 mm, an accelerating voltage of 15 kV, and a chamber pressure of 9–10 Torr were suitable for obtaining high-resolution images.

### Bioassays

Human erythrocytes were obtained from healthy donors. The whole blood was taken into ethylenediaminetetraacetic acid anticoagulant. After extraction, the blood was centrifuged (3000 r.p.m. for 5 min) to remove plasma and leukocyte layer, washed three times with phosphate buffer saline solution (137 mM NaCl, 2.7 mM KCl, 1.5 mM  $\text{KH}_2\text{PO}_4$ , and 8 mM  $\text{Na}_2\text{HPO}_4$ ), and centrifuged again. Erythrocytes were re-suspended in saline solution (0.9% NaCl) to get a concentration of  $\sim 10^7$  human red blood (HRB) cells/mL.<sup>[23]</sup> In all experiments, erythrocytes were used immediately after isolation.

The erythrocyte suspensions (2 mL,  $\sim 10^7$  HRB cells/mL) in glass tubes (1.5 × 10 cm) were dark-incubated with HGs of different composition for 24 hr. Then, the tubes were centrifuged and 100  $\mu$ L of the supernatants was diluted in 2 mL of distilled water. The hemoglobin content was determined by measuring the absorbance at 413 nm ( $A_{\text{hem}}$ ). The results are expressed as percentage of hemolysis [eqn (3)] taking the absorbance obtained from a sample lysed in distilled water as 100% ( $A_{100\%}$ ).<sup>[24]</sup> A blank was performed without HG addition ( $A_b$ ).

$$\text{Hemolysis \%} = \frac{A_{\text{hem}} - A_b}{A_{100\%} - A_b} \times 100 \quad (3)$$

## RESULTS AND DISCUSSION

### Synthesis of hydrogels

Figure 2(a) shows the absorption spectra of Saf, ASA, and Ibu in aqueous solution. The emission spectrum of the green LEDs, used as radiation source to conduct the photopolymerization reaction, is also shown. Saf is the only species that absorbs the green light of the LEDs, and its absorption spectrum completely overlaps the emission spectrum of the LEDs. The fact that no polymerization reaction occurred in the absence of SFMA proves its role as co-initiator of the photopolymerization, in addition to its participation as a crosslinker.

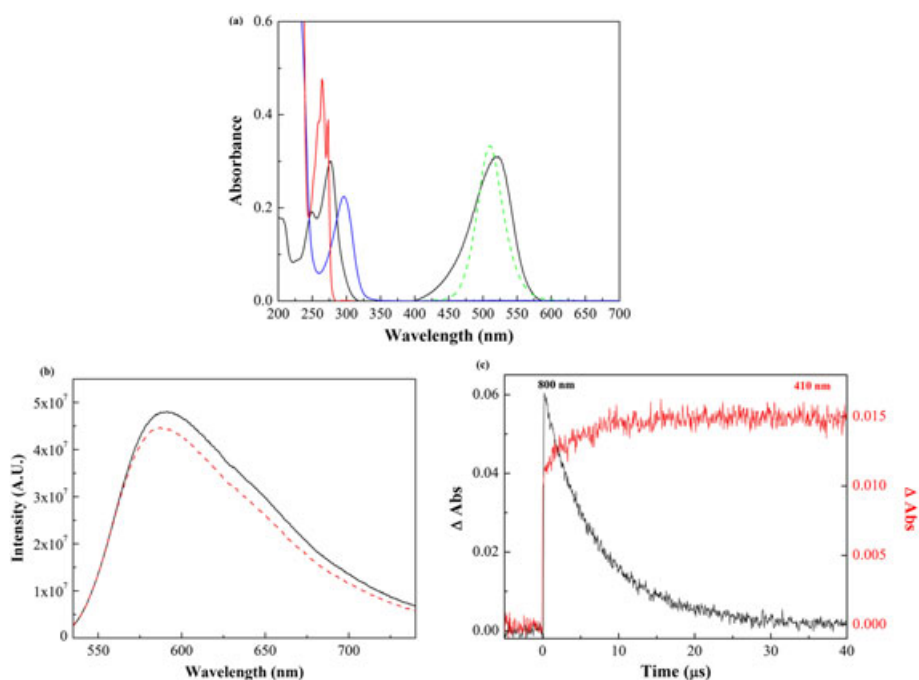


**Figure 2.** Photophysical characterization of the photoinitiator system. (a) UV-Vis spectra of Saf (—), ASA (—), and Ibu (—). Emission spectrum of green LEDs employed in the photopolymerization reaction (dashed line). (b) Fluorescence emission spectra of aqueous solutions of Saf (—) and Saf/SFMA (---). [Saf]:  $1 \times 10^{-5}$  M; [SFMA]:  $4.5 \times 10^{-3}$  M; excitation wavelength: 525 nm. (c) Transient absorption at 410 and 800 nm for Saf:  $1 \times 10^{-5}$  M in the presence of SFMA:  $4.5 \times 10^{-3}$  M.

Because the drugs used have no absorption in the visible region of the spectrum (Fig. 1), the green light emission of LEDs, employed in the polymerization reaction, avoids any kind of photodegradation reactions that involve excited states of Ibu and ASA, and therefore should not affect their therapeutic action. This was confirmed by the fact that their UV-Vis spectra were the same compared with the individual drugs in solution, when they were extracted from the HGs. Table 1 shows the compositions of the synthesized HGs and the experimental conditions employed in the synthesis.

After irradiation, the samples were allowed to stabilize for 48 hr in the dark. HGs were cut in uniform disks and dried in an oven at 40°C for 48 hr.

**Table 1.** Composition of synthesized materials

HG abbreviation	% SFMA (in weight)	Drug (10 mg/g polymer)
HG-0.5	0.5	None
HG-1	1	None
HG-2	2	None
HG-0.5 ASA	0.5	ASA
HG-2 ASA	2	ASA
HG-0.5 Ibu	0.5	Ibu
HG-2 Ibu	2	Ibu

Volume irradiated: 3 ml; purged: 15 min with Ar; irradiation source: 12 green LEDs ( $\lambda_{\text{max}} \sim 530$  nm); irradiation time: 3 hr; temperature: ambient conditions ( $\sim 20^\circ\text{C}$ ); stabilization time: 72 hr.

### Analysis of the photoinitiation mechanism

Figure 2(b) shows the emission spectra of Saf and Saf/SFMA in aqueous solution. Absorption and emission spectra of Saf are highly dependent on the polarity of the solvent.<sup>[25]</sup> The small red shift in the ground state absorption and the blue shift in the emission band are a characteristic signature of a decrease in solvent polarity. Despite the small concentration of SFMA in the dye solution, this behavior could be ascribed to a preferential solvation of Saf by SFMA molecules.<sup>[26]</sup> We can therefore infer that the aqueous solution of SFMA is equivalent to a less polar solvent for Saf.

A mechanism of generation of radicals using Saf as sensitizer and SFMA as co-initiator was proposed in our previous study.<sup>[19]</sup> In this mechanism, the active amino radicals are produced by an electron transfer reaction between deprotonated excited states of the dye (Saf<sup>1,3</sup>) and the amine. This reaction leads to the formation of semi-reduced Saf in the form of a radical anion and the radical cation of the amine. The latter undergoes a second fast proton transfer, leading to an active radical that initiates the polymerization.

The quenching rates of singlet and triplet states of the dye in the presence of SFMA were determined. It is well known that aliphatic amines quench the excited states of Saf.<sup>[22,27,28]</sup> Therefore, it is expected that the secondary amine groups present in SFMA should quench excited states of Saf. In fact, a small quenching of the emission of Saf produced by the presence of SFMA can be observed in the stationary fluorescence spectra reported in Fig. 2. The quenching of the singlet state of Saf by SFMA in aqueous solution was determined by fluorescence lifetime measurements. The singlet quenching rate constant, obtained by Stern–Volmer analysis, was  $1.60 \times 10^9 \text{ M}^{-1} \text{ sec}^{-1}$ .

The triplet state quenching of the dye by SFMA was investigated by laser flash photolysis by monitoring the decay at



800 nm, the wavelength corresponding to pure triplet–triplet absorption of Saf in water.<sup>[29]</sup> The resulting bimolecular quenching rate constant was  $2.50 \times 10^7 \text{ M}^{-1} \text{ sec}^{-1}$ , a value lying in the range of quenching rate constants previously reported for the quenching of Saf by aliphatic amines.<sup>[22]</sup>

However, at the SFMA concentrations employed, the fraction of singlet state of the dye quenched by SFMA was less than 1% while the fraction of triplet state quenched by SFMA was around 90%. Therefore, the main contribution to the generation of active amino radicals resulted from the electron transfer reaction between the excited triplet state of the dye and SFMA.

Figure 2(c) shows the temporal evolution of both transient absorptions: the triplet excited state of Saf (absorbance at 800 nm) and that of the corresponding radical anion (absorbance at 410 nm), generated in the presence of SFMA ( $4.5 \times 10^{-3} \text{ M}$ ). The initial absorption at 410 nm can be ascribed to the triplet state of the dye.<sup>[29]</sup> The subsequent growth matches the triplet decay and corresponds to the radical anion formed in the triplet state quenching process.

When Saf was continuously irradiated near the maximum of its absorption band in the presence of SFMA, a photobleaching process took place. The photobleaching kinetics was studied by actinometry, monitoring the relative change in the dye absorbance with irradiation time.<sup>[28,30]</sup> The photoreaction quantum yield, determined for Saf in the presence of SFMA 0.06 M, was 0.031. However, during the photopolymerization, monomers act as efficient inhibitors of the photobleaching of the dye, as observed previously.<sup>[22]</sup> This protective effect can be ascribed to the fast transfer of generated radicals to monomers, initiating the chain polymerization. Photophysical parameters are summarized in Table 2.

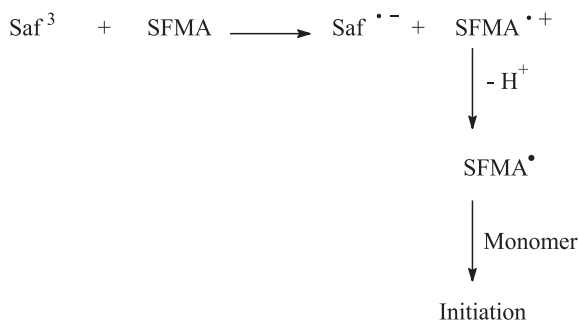
The photoinitiation mechanism is indicated in Scheme 1.

### Effect of SFMA content and pH on the swelling of HG

Swelling behavior of HGs containing different amounts of SFMA, at pH=7 and 25°C, is represented in Fig. 3(a). The swelling

**Table 2.** Photophysical parameters for Saf in the presence of SFMA (water)

Parameter	Value
$\lambda_{\text{max}}$ (Abs)	523 nm
$\lambda_{\text{max}}$ (Flu)	587 nm
$^1k_{\text{q}}$	$1.60 \times 10^9 \text{ M}^{-1} \text{ sec}^{-1}$
$^3k_{\text{q}}$	$2.50 \times 10^7 \text{ M}^{-1} \text{ sec}^{-1}$
$\Phi_{\text{pb}}$	0.031



**Scheme 1.** Mechanism of photogeneration of active amino radicals.

degree at equilibrium decreased when increasing the amount of crosslinker: HG-0.5 > HG-1 > HG-2. These results can be interpreted with the Flory–Rehner equation,<sup>[30]</sup> which determines that the degree of swelling is inversely proportional to the crosslink density. As can be observed in Fig. 3(a), increasing the amount of crosslinker led to a faster swelling rate even though the final value was lower. The faster swelling rate may be ascribed to the hydrophilic character of SFMA produced by the presence of secondary amines, hydroxyls, and silanol groups in its structure (Fig. 1).

The effect of pH on the swelling degree at different pH values for HG-0.5 is represented on Fig. 3(b). The inset shows the effect of SFMA concentration in the swelling of HGs at different pHs. An increase in the swelling degree was observed with the increase in pH values for all synthesized formulations. This behavior was explained by the hydrolysis of amide groups of the polymer chain at high pH values.<sup>[20]</sup>

Scanning electron microscope micrographs are useful to reveal the HGs structure, although it is necessary take into account the fact that dehydration conditions and/or fixation procedures may affect the observed morphology.<sup>[31]</sup>

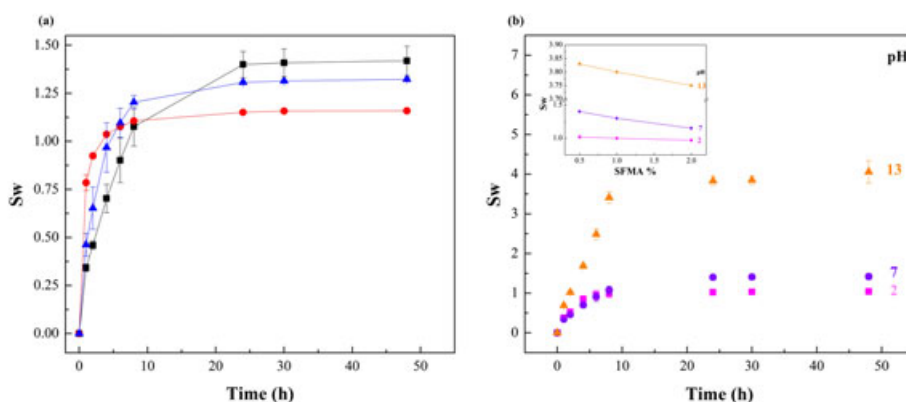
The SEM micrographs of HGs with different contents of SFMA, swollen 24 hr in buffer solutions to the equilibrium value, are shown in Fig. 4. The presence of compact areas without pores (decrease in porosity) is observed when increasing the crosslinker amount. Besides, by increasing the pH, an increase in number and size of pores is observed.

Table 3 summarized equilibrium swelling ratios of the different HGs at 25 and 40°C and pH = 7. In the equilibrium conditions, HGs at 40°C follow the same behavior of that observed at 25°C; swelling capacity declines with increase the percentage of SFMA. However, by comparison of swelling at 25 and 40°C, it is appreciable that at equilibrium, swelling diminishes with the increment of temperature.

As discussed previously, increasing the crosslinker amount led to a decrease in the equilibrium swelling ratio. A second effect, not investigated here, is the simultaneous increase in mechanical properties. For example, Johnson *et al.* showed that varying the crosslinker concentration in HEMA–acrylic acid HGs was an effective method of controlling mechanical properties.<sup>[32]</sup>

The effect of temperature was more significant for samples with lower crosslink density and was practically negligible (in fact opposite) for the sample with the highest crosslink density. Changes in hydrophobic–hydrophilic balance and a reduction in the fraction of H-bonds are induced by increasing temperature. The thermal response of certain HGs is a property of interest because when active principles are incorporated to these materials, they can be released to the media in response to an external stimulus such as temperature.<sup>[12]</sup>

The swelling results were fitting according to eqn (1). The diffusional exponent values,  $n_p$ , and the corresponding correlation coefficient  $R$  are summarized in Table 3;  $n_p$  is often used to determine the transport mechanism mode. For  $n_p < 0.5$ , the swelling behavior fits Fickian diffusion, in which the water transport is governed by a simple concentration gradient. For  $0.5 < n_p < 1$ , the water uptake conforms to an anomalous diffusion, where the water uptake is controlled collaboratively by HGs relaxation and water diffusion (non-Fickian diffusion). For  $n_p > 1$ , the controlled relaxation of the polymer chain dominates the water transport (anomalous diffusion).<sup>[21]</sup> According to the results in Table 3, within experimental error, all formulations at 25 and 40°C present  $n_p$  values lower than or near to



**Figure 3.** (a) Effect of SFMA concentration on swelling capacity of HG-0.5, HG-1, and HG-2 at pH = 7 and 25°C for HG-0.5 (▲), HG-1 (■), and HG-2 (●). (b) Effect of pH on swelling of HG-0.5. Inset: effect of SFMA concentration on the swelling of HG-0.5, HG-1, and HG-2 at pH 2 (●), 7 (●), and 13 (▲). Data represent the mean ± SD from at least three independent measurements.

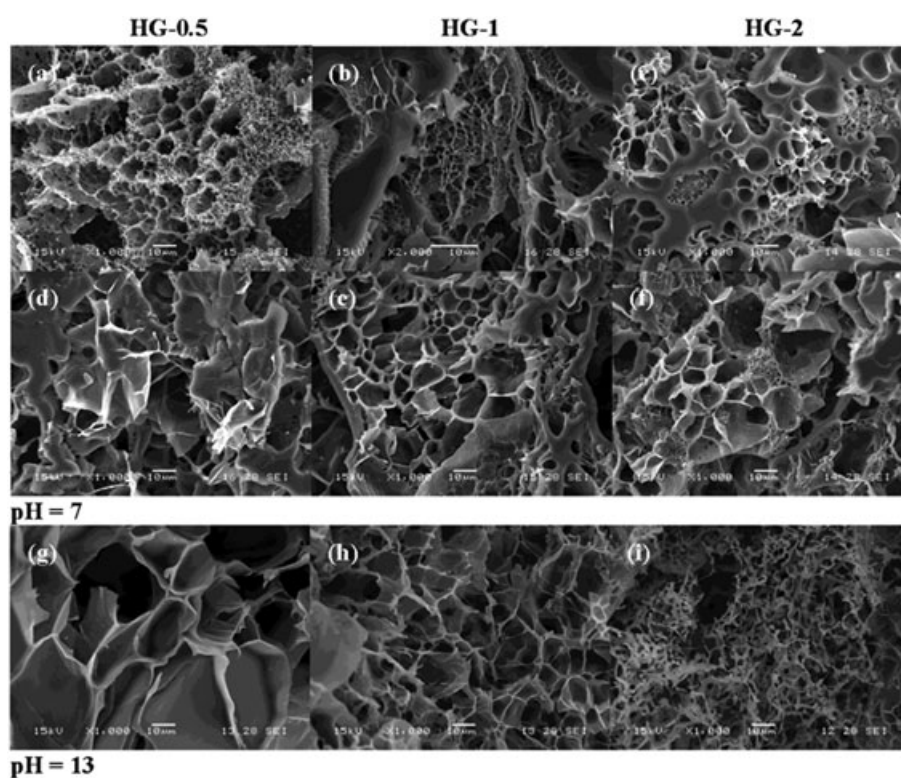


**Figure 4.** SEM micrographs of HGs with different contents of SFMA, swollen to the equilibrium value (24 hr in buffer) at pH = 7 (a–f) and at pH = 13 (g–i) at 25°C. HG-0.5 (a, d, and g), HG-1 (b, e, and h), and HG-2 (c, f, and i).

0.5; this indicated that the water transport followed Fickian swelling process dominated by free diffusion of water. As expected,  $n_p$  values increase according SFMA content decrease and are higher at 25 than at 40°C.

#### Study of hemolytic activity of HG on HRB cells

The biological membranes of HRB cells can be an important target for many drugs. In this sense, the erythrocytes are considered an attractive and suitable model system to study membrane modification. Damage of HRB cells produces a significant increase of membrane fluidity due to the formation of defects in the cell membrane. This effect decreases the osmotic

stability of erythrocytes and produces the release of hemoglobin. Thus, HRB cells were used to evaluate the cytotoxic

**Table 3.** Swelling properties of HGs at pH = 7

HG	Temperature	ESR	$n_p$	$R$
HG-0.5	25°C	1.4190	0.56	0.992
HG-1	25°C	1.3233	0.47	0.986
HG-2	25°C	1.1590	0.20	0.979
HG-0.5	40°C	1.2491	0.47	0.987
HG-1	40°C	1.2195	0.28	0.986
HG-2	40°C	1.1715	0.12	0.999

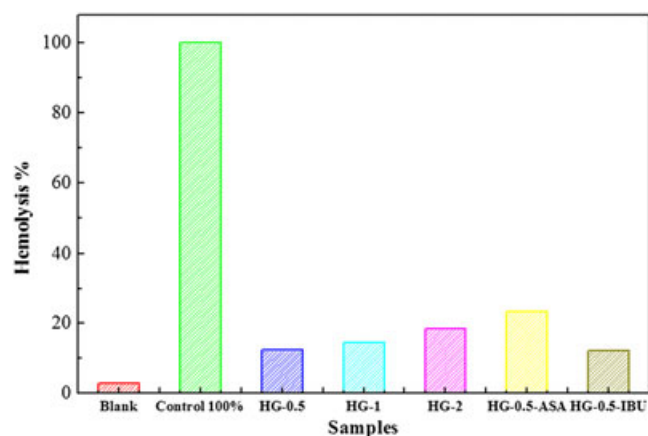


**Figure 5.** Hemolytic effect of HG over HRB cells incubated 24 hr in the dark.

activity of different drugs.<sup>[33]</sup> *In vitro* activity of HG was determined by hemolytic effect on HRB cells for five of the formulations (Fig. 5).

In accordance with cell-culture assays, where cell death is monitored by membrane disruption, hemolysis of red blood cells can be regarded as a mode of measuring death of erythrocytes.<sup>[34]</sup> In this assay, the cytotoxicity produced by HG of different compositions, upon erythrocyte cells, was evaluated. The observed hemolysis was the result of both the HGs and the loaded drug.

Figure 5 shows that hemolysis increases with the SFMA contents. In a recently published paper, the results revealed that silica particles cause hemolysis in a degree that depends on their size and concentration. This behavior was attributed to the presence of silanol groups.<sup>[35]</sup> In fact, we also note that the hemolytic activity increases with increasing SFMA concentration in HGs, which could also be ascribed in this case to the increment of silanol groups in the polymeric network.

On the other hand, Fig. 5 shows that greater hemolysis is observed when HGs release ASA. This result was expected because ASA is known to produce hemolysis of erythrocytes.<sup>[36]</sup> In spite of this, ASA is a drug commonly used worldwide. Similar results are observed for Ibu.

In order to employ these materials in biological applications, hemolytic characteristics could be improved after surface modification, as proposed in the literature.<sup>[35]</sup>

## Release experiments

Drug-release measurements were carried out at 25°C in buffer solutions of pH = 7 or 10. Figure 6 shows the cumulative fractional release (CFR) percentage of ASA and Ibu versus time.

Data in Fig. 6(a) show that the drug release rates increased rapidly during the first 8 hr of the experiment and then they gradually slowed down. The quick release of the drug from the carrier in the early stage of the experiment was attributed to the burst effect. It is a known fact that the HG has to swell to a certain extent before it can release its contents and the resultant effect is the fast release of the solute in a short span of time, after which further release is diffusively controlled.

At pH 7, the fractional release of ASA was practically independent of the crosslink density of the HG. At pH 10, the release was significantly faster and the rate increased with the amount of SFMA in the HGs. The variation of release rate with crosslink density was unexpected because a faster release rate should be observed when increasing the porosity (swelling ratio) of the HGs. A possible explanation of this effect is the decrease of the fraction of hydrogen bonds between carboxylic groups of ASA and secondary amine groups of SFMA, produced by partial formation of carboxylate groups at pH 10 (pKa of ASA is 3.49<sup>[37]</sup>). This could be the prevailing effect instead of porosity. In any case, the significant dependence of release rate on pH may be used for practical drug-delivery applications.

Figure 6(b) shows the experimental results obtained for the release of Ibu. Trends are similar than those observed for ASA. The difference is that in the case of Ibu, the release rate was faster for the less crosslinked HGs, as expected (pKa of Ibu is 4.4<sup>[38]</sup>). Again,

**Table 4.** Drug released from HG in different media containing NSAID at 25°C

HG	pH	$M_{24h}$ (mass %)	$n$	$D$ (cm <sup>2</sup> sec <sup>-1</sup> )	$R$
HG-0.5 ASA	7	74.20	0.58	$1.93 \times 10^{-8}$	0.999
HG-2 ASA	7	69.29	0.60	$1.15 \times 10^{-8}$	0.992
HG-0.5 ASA	10	84.96	0.40	$1.12 \times 10^{-6}$	0.996
HG-2 ASA	10	97.36	0.52	$2.60 \times 10^{-7}$	0.999
HG-0.5 Ibu	7	65.32	0.56	$1.84 \times 10^{-8}$	0.972
HG-2 Ibu	7	54.22	0.65	$1.08 \times 10^{-9}$	0.988
HG-0.5 Ibu	10	99.87	0.41	$9.53 \times 10^{-7}$	0.983
HG-2 Ibu	10	80.79	0.42	$7.08 \times 10^{-7}$	0.993

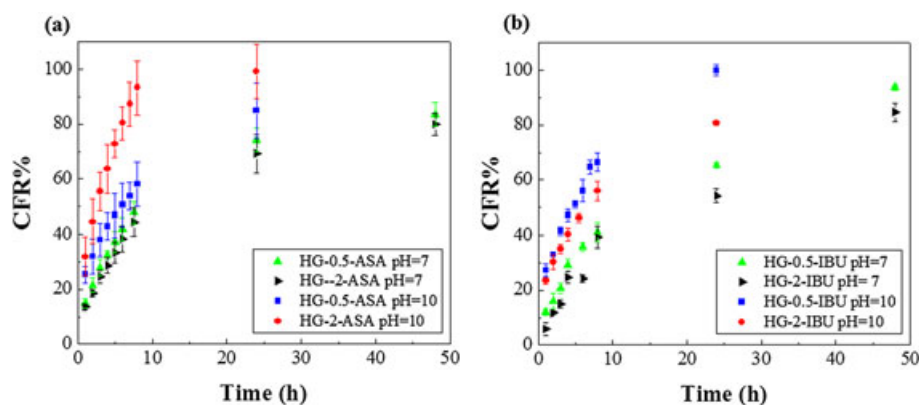


**Figure 6.** Release experiments. (a) Release of ASA from HG-0.5 and HG-2, at 25°C, and pH 7 or 10. (b) Release of Ibu from HG-0.5 and HG-2, at 25°C, and pH 7 or 10. Data represent the mean  $\pm$  SD from at least three independent measurements.



the significant dependence of release rate on pH may be used for practical applications.

The semi-empirical power law [eqn (2)] developed by Peppas *et al.*<sup>[21]</sup> was employed to model the *in vitro* drug release kinetic of ASA and Ibu. When the value of the exponent is  $n < 0.5$ , the release rate follows Fick's law. For systems following a Fickian behavior, diffusion coefficients ( $D$ ) may be calculated from the slope of the plot of  $M_t/M_\infty$  versus  $t^{1/2}$ ; the initial slope is equal to  $4D^{1/2}/\pi^{1/2}L$ , where  $L$  is the slab thickness.<sup>[39]</sup> When  $0.5 < n < 1$ , it is an anomalous diffusion.<sup>[40]</sup>

Table 4 contains the mass percentage of NSAID release at 24 hr ( $M_{24h}$ ) and  $n$  and  $R$  values obtained from the linearization of eqn (2) and the values of  $D$ . All data could be fitted with reasonably high correlation coefficient values.

As observed from Table 4, both NSAIDs studied present values of  $n$  near 0.5. The diffusion coefficient reported in Table 3 lies in the same range as some of the values reported in the literature.<sup>[20,39,40]</sup>

## CONCLUSIONS

The photoinitiation mechanism of the radical copolymerization of HEMA and AAm, in the presence of Saf (initiator)/SFMA (co-initiator/crosslinker), was investigated. The mechanism was based on the deactivation of both singlet and triplet excited states of Saf by an electron transfer reaction to SFMA, with deactivation rate constants of  $1.60 \times 10^9$  and  $2.50 \times 10^7 \text{ M}^{-1} \text{ s}^{-1}$ , respectively. The main contribution involved the deactivation of the triplet excited state. This led to the formation of semi-reduced Saf in the form of a radical anion and the radical cation of the amine. A fast proton transfer from the radical cation to the radical anion generates an active radical that initiates the polymerization. The photoreaction quantum yield for the reaction between SFMA and Saf was 0.031.

Two different drugs, ASA and Ibu, were loaded in the HG during the synthesis. Release rates of these drugs depended on pH and on the amount of SFMA used in the synthesis. Increasing the pH from 7 to 10 produced a significant increase of the release rate of both drugs. This was ascribed to the increase in the partial ionization of the carboxylic acid groups present in both components. This reduced the interactions with the secondary amine groups present in SFMA and increased the release rate. The effect was larger for ASA ( $pK_a = 3.49$ ) than for Ibu ( $pK_a = 4.4$ ). Increasing the amount of SFMA increased both the crosslink density and the fraction of H-bonds formed with the drugs. At pH 10, the first effect was dominant for the release of Ibu while the second effect determined the release rate of ASA. Both variables, SFMA amount and pH, can be selected to control the release rate of both drugs. These systems did not exhibit significant toxicity effects making them appropriate for practical applications.

## Acknowledgements

All authors are members of Consejo Nacional de Investigación Científica y Tecnológica (CONICET). A. Gallastegui thanks CONICET for graduate fellowship. The financial support of Universidad Nacional de Río Cuarto (Res. Rec 161/16), Consejo Nacional de Investigación Científica y Tecnológica (PIP 2015/2017 Cod. 11220150100295CO), and Agencia Nacional de Promoción Científica y Tecnológica (PICT-2013-1439) from Argentina is gratefully acknowledged.

## REFERENCES

- [1] G. Jiménez López, F. Debasa García, T. Bastanzuri Villares, J. Pérez Peña, J. Ávila Pérez, *Rev. Cubana Farm.* **2003**, *37*, 1561–1588.
- [2] G. F. Longstreth, *Am. J. Gastroenterol.* **1995**, *90*(2), 206–210.
- [3] S. P. Gutthann, L. A. García Rodríguez, D. S. Raiford, *Epidemiology* **1997**, *8*(1), 18–24.
- [4] G. T. Carter, V. Duong, S. Ho, K. C. Ngo, C. L. Greer, D. L. Weeks, *Phys. Med. Rehabil. Clin. N. Am.* **2014**, *25*, 457–470.
- [5] S. W. Song, K. Hidajat, *Langmuir* **2005**, *21*, 9568–9575.
- [6] Y. B. Lu, W. B. Sun, Z. Gu, *J. Control. Rel.* **2014**, *194*(28), 1–19.
- [7] S. De Robertis, M. C. Bonferoni, L. Elviri, G. Sandri, C. Caramella, R. Bettini, *Expert Opin. Drug Del.* **2015**, *12*(3), 441–453.
- [8] M. A. Lago, V. Y. Grinberg, T. V. Burova, A. Concheiro, C. Alvarez-Lorenzo, *J. Funct. Biomater.* **2011**, *2*, 373–390.
- [9] J. D. Andrade, Hydrogels for medical and related applications. ACS Symposium Series, American Chemical Society, Washington, DC, **1976**.
- [10] E. Mathiowitz, Encyclopedia of controlled drug delivery. Wiley-Interscience Publications, USA, Volumes 1–2, **1999**.
- [11] R. Barbucci, *Hydrogels. Biological Properties and Applications*. Springer-Verlag Italia SRL, Milan, **2009**.
- [12] I. Galaev, B. Mattiasson, SMART POLYMERS, *Applications in Biotechnology and Biomedicine*, Second edn. . CRC Press, USA, **2008**.
- [13] R. M. Ottenbrite, K. Park, T. Okano, *Biomedical Applications of Hydrogels Handbook*. Springer, London, **2010**.
- [14] R. Yoyida, T. Okano, Y. Sakurai, K. Sakai, *J. Biomater. Sci. Polym.* **1994**, *6*, 585–598.
- [15] J. D. Andrade, Hydrogels for medical and related applications. ACS Symposium Series, Washington DC, **1976**.
- [16] J. M. Wood, D. Attwood, J. H. Collet, *J. Pharm. Pharmacol.* **1982**, *34*, 1–4.
- [17] J. Shao, Y. Huang, Q. Fan, *Polym. Chem.* **2014**, *5*, 4195–4210.
- [18] T. -Y. Liu, S. -Y. Chen, Y. -L. Lin, D. -M. Liu, *Langmuir* **2006**, *22*, 9740–9745.
- [19] M. L. Gomez, D. P. Fasce, R. J. J. Williams, R. Erra-Balsells, M. K. Fatema, H. Nonami, *Polymer* **2008**, *49*, 3648–3653.
- [20] M. L. Gomez, R. J. J. Williams, H. A. Montejano, C. M. Previtali, *eX-PRESS Polym. Lett.* **2012**, *6*, 189–197.
- [21] P. L. Ritger, N. A. Peppas, *J. Control. Release* **1987**, *5*, 23–36.
- [22] M. L. Gómez, V. Avila, H. A. Montejano, C. M. Previtali, *Polymer* **2003**, *44*, 2875–2881.
- [23] M. B. Spesia, M. Rovera, E. N. Durantini, *Eur. J. Med. Chem.* **2010**, *45*, 2198–2205.
- [24] M. Hoebke, H. J. Schuitmaker, L. E. Jannink, T. M. A. R. Dubbelman, A. Jakobs, A. Van de Vorst, *Photochem. Photobiol.* **1997**, *66*, 502–508.
- [25] M. L. Gómez, C. M. Previtali, H. A. Montejano, *Spectrochim. Acta, Part A: Chem.* **2004**, *60*, 2433–2439.
- [26] C. Reichardt, *Solvents and Solvent Effects in Organic Chemistry*, Third edn. . Wiley — VCH, Germany, **2003**.
- [27] M. V. Encinas, A. M. Rufs, M. G. Neumann, C. M. Previtali, *Polymer* **1996**, *37*, 1395–1398.
- [28] C. M. Previtali, S. G. Bertolotti, M. G. Neumann, I. A. Pastre, A. M. Rufs, M. V. Encinas, *Macromolecules* **1994**, *27*, 7454–7458.
- [29] C. E. Baumgartner, H. H. Richtol, D. A. Aikens, *Photochem. Photobiol.* **1981**, *34*, 17–22.
- [30] P. J. Flory, J. Rehner, *J. Chem. Phys.* **1943**, *11*, 521–526.
- [31] P. D. Hong, J. H. Chen, *Polymer* **1998**, *32*, 5809–5817.
- [32] B. D. Johnson, D. J. Beebe, W. C. Crone, *Mater. Sci. Eng. C* **2004**, *24*, 575–581.
- [33] A. A. Fariheen, N. A. Shaikh, M. Riaz, *Toxicol. in Vitro* **2015**, *29*, 1878–1886.
- [34] J. Viskupicova, D. Blaskovic, S. Galiniak, M. Soszyński, G. Bartosz, L. Horakova, I. Sadowska-Bartos, *Redox Biol.* **2015**, *5*, 381–387.
- [35] I. S. Lin, C. L. Haynes, *J. Am. Chem. Soc.* **2010**, *132*, 4834–4842.
- [36] N. T. Shahidi, D. W. Westring, *J. Clin. Invest.* **1970**, *49*, 1334–1340.
- [37] D. Cairns, *Essentials of Pharmaceutical Chemistry*, Fourth edn. . Pharmaceutical Press, London, **2012**.
- [38] T. Ahmad, B. Srihari, B. Alresheedi, N. M. Gowda, *Int. J. Appl. Sci. Tech.* **2012**, *2*, 49–56.
- [39] S. L. Tomić, S. I. Dimitrijević, A. D. Marinković, S. Najman, J. M. Filipović, *Polym. Bull.* **2009**, *63*, 837–851.
- [40] L. Masaro, X. X. Zhu, *Prog. Polym. Sci.* **1999**, *24*, 731–775.